

## Perturbation of the Fe–O<sub>2</sub> Bond by Nearby Residues in Heme Pocket: Observation of $\nu_{\text{Fe-O}_2}$ Raman Bands for Oxy-myoglobin Mutants

Shun Hirota,<sup>†‡</sup> Tiansheng Li,<sup>‡</sup> George N. Phillips, Jr.,<sup>‡</sup> John S. Olson,<sup>\*‡</sup> Masahiro Mukai,<sup>‡</sup> and Teizo Kitagawa<sup>\*‡</sup>

Institute for Molecular Science  
Okazaki National Research Institutes  
Myodaiji, Okazaki, 444 Japan  
Department of Biochemistry and Cell Biology and  
The W. M. Keck Center for Computational Biology  
Rice University, Houston, Texas 77005-1892

Received March 13, 1996

Elucidation of Fe–O<sub>2</sub> and O<sub>2</sub>–protein interactions in oxygenated heme proteins has been the focus of a large number of structural and spectroscopic studies. X-ray crystallographic analysis on oxymyoglobin (O<sub>2</sub>Mb) suggested the presence of a hydrogen bond between the distal histidine (His-64) and bound O<sub>2</sub>; a proposal was later confirmed in neutron diffraction experiments.<sup>1</sup> Vibrational spectroscopy, including infrared (IR) absorption and resonance Raman (RR) scattering, has provided more detailed information on protein ligand interactions.<sup>2a–c,e,g</sup> Yu and co-workers<sup>2a</sup> suggested that the Fe–CO stretching ( $\nu_{\text{Fe-CO}}$ ) frequency depends on the Fe–C–O bond angle and accordingly reflects steric hindrance from nearby residues. More recent work has indicated that the electrostatic field near bound CO exerts a greater influence on the polarization of CO and its  $\nu_{\text{Fe-CO}}$  frequency than does steric hindrance.<sup>2d–g</sup>

The Fe–O<sub>2</sub> complexes of Mb and hemoglobin (Hb) mutants have been much less studied, compared with their CO adducts, because of autoxidation problems. Since the O–O stretching mode ( $\nu_{\text{OO}}$ ) couples with internal modes of the trans ligand (histidine),<sup>3</sup> it is difficult to deduce the intrinsic  $\nu_{\text{OO}}$  frequencies from the observed frequencies. The Fe–O<sub>2</sub> stretching ( $\nu_{\text{Fe-O}_2}$ ) mode has been identified for several end-on type O<sub>2</sub>-bound heme proteins by RR spectroscopy,<sup>4</sup> and its observed frequency directly reflects the strength of the Fe–O<sub>2</sub> bond. We report here the  $\nu_{\text{Fe-O}_2}$  Raman bands for His-64 → Leu (H64L), Leu-29 → Phe (L29F), and Leu-29 → Trp (L29W) mutants of sperm whale Mb and discuss the effects of these residues on the Fe–O<sub>2</sub> vibration.

\* Author to whom correspondence should be addressed.

† Present address: Department of Chemistry, Faculty of Science, Nagoya University, Chikusa-ku, Nagoya, 464-01, Japan.

‡ Okazaki National Research Institutes.

‡ Rice University.

(1) Phillips, S. E.; Schoenborn, B. P. *Nature* **1981**, 292, 81–82.

(2) (a) Yu, N.-T.; Kerr, E. A.; Ward, B.; Chang, C. K. *Biochemistry* **1983**, 22, 4534–4540. (b) Ray, G. B.; Li, X. Y.; Ibers, J. A.; Sessler, J. L.; Spiro, T. G. *J. Am. Chem. Soc.* **1994**, 116, 162–176. (c) Sakan, Y.; Ogura, T.; Kitagawa, T.; Fraunfelder, F. A.; Mattern, R.; Ikeda-Saito, M. *Biochemistry* **1993**, 32, 5815–5824. (d) Auspurger, J. D.; Dykstra, C. E.; Oldfield, E. *J. Am. Chem. Soc.* **1991**, 113, 2447–2451. (e) Li, T.; Quillin, M. L.; Phillips, G. N., Jr.; Olson, J. S. *Biochemistry* **1994**, 33, 1433–1446. (f) Jewsbury, P.; Kitagawa, T. *Biophys. J.* **1994**, 67, 2236–2250. (g) Nakashima, S.; Olson, J. S.; Mukai, M.; Kitagawa, T. to be submitted.

(3) Proniewicz, L. M.; Bruha, A.; Nakamoto, K.; Uemori, Y.; Kyuno, E.; Kincaid, J. R. *J. Am. Chem. Soc.* **1991**, 113, 9100–9104.

(4) (a) Brunner H. *Naturwissenschaften*, **1974**, 61, 129. (b) Nagai, K.; Kitagawa, T.; Morimoto, H. *J. Mol. Biol.* **1980**, 136, 271–289. (c) Duff, L. L.; Appelman, E. H.; Shriver, D. F.; Klots, I. M. *Biochem. Biophys. Res. Commun.* **1979**, 90, 1098–1103. (d) Kerr, E. A.; Yu, N.-T.; Bartnicki, D. E.; Mizukami, H. *J. Biol. Chem.* **1985**, 260, 8360–8365. (e) Hu, S.; Schneider, A. J.; Kincaid, J. R. *J. Am. Chem. Soc.* **1991**, 113, 4815–4822. (f) Van Wart, H. E.; Zimmer, J. *J. Biol. Chem.* **1985**, 260, 8372–8377. (g) Ogura, T.; Takahashi, S.; Shinzawa-Itoh, K.; Yoshikawa, S.; Kitagawa, T. *J. Am. Chem. Soc.* **1990**, 112, 5630–5631. (h) Hirota, S.; Ogura, T.; Appelman, E. H.; Shinzawa-Itoh, K.; Yoshikawa, S.; Kitagawa, T. *J. Am. Chem. Soc.* **1994**, 116, 10564–10570.

Preparation of mutant Mbs has been described elsewhere.<sup>2c</sup> The purified protein was dissolved in 50 mM Na-phosphate buffer, pH 7.4. Crystals of L29W MbO<sub>2</sub> were grown in the P6 form using 2.2 to 2.6 M ammonium sulfate, 20 mM Tris-HCl, 1 mM EDTA.<sup>5a</sup> Diffraction data were collected on a Rigaku R-axis IIC imaging plate. The number of unique reflections was 17 658, and the starting model for molecular replacement was L29F MbO<sub>2</sub>.<sup>5c</sup> Constrained least-squares refinement was performed by X-PLOR. After nine cycles of refinement and solvent placement, the crystallographic R-factor converged to 15.8%, with a final resolution of 1.8 Å and 77.5% completeness. The coordinates and structure factors are being submitted to the Brookhaven Protein Data Bank.

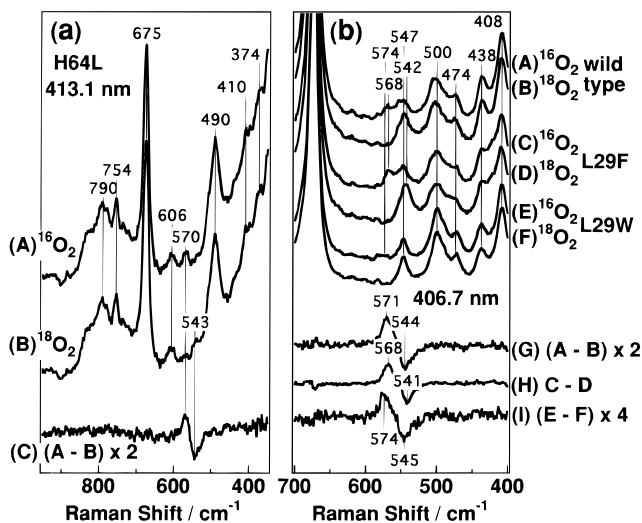
In order to observe the  $\nu_{\text{Fe-O}_2}$  Raman band of unstable oxy species, we used the oxygenation system originally developed for studies of cytochrome *c* oxidase.<sup>6</sup> About 20 mL of CO-bound Mb (10  $\mu$ M) was circulated through the system at a flow rate of 20 mL/min. Oxygen (<sup>16</sup>O<sub>2</sub> or <sup>18</sup>O<sub>2</sub>) was incorporated into the solution just before the quartz Raman cell (cross section = 0.6 × 0.6 mm<sup>2</sup>). Two laser beams, which were obtained from a single Kr<sup>+</sup> laser (Spectra Physics, Model 2016), but separated with a prism, were focused on the flow cell. One laser beam, at the upstream side (406.7 nm, 20 mW), photodissociates CO from COMb. O<sub>2</sub> competitively binds to the photodissociated deoxyMb due to its larger binding rate.<sup>5a,b</sup> Raman scattering from the O<sub>2</sub>-bound hemes is excited with the other laser beam (413.1 nm, 2 mW), which is located 100  $\mu$ m on the downstream side from the 406.7 nm beam. With the flow rates employed, the O<sub>2</sub> adduct is monitored at 0.1 ms after CO-photodissociation. The heme is quickly oxidized after O<sub>2</sub> binding, but its Raman spectrum is observed before autoxidation. The original reduced CO-bound form is restored from the autoxidized Mb during one cycle of the circulation system.<sup>6</sup>

Figure 1(a) shows the RR spectra in the 950 to 350 cm<sup>-1</sup> region for the <sup>16</sup>O<sub>2</sub> (A) and <sup>18</sup>O<sub>2</sub> (B) adducts of the H64L mutant Mb excited at 413.1 nm. The band at 490 cm<sup>-1</sup> arises from the  $\nu_{\text{Fe-CO}}$  mode of recombined and unphotolyzed COMb, whose frequency is in agreement with the values reported for the equilibrium form of COMb.<sup>2c,g</sup> Since the  $\nu_{\text{Fe-CO}}$  Raman band is considerably enhanced in intensity near the Soret region, the band appears strong even if its concentration is relatively low. A band at 570 cm<sup>-1</sup> in spectrum A is shifted to 543 cm<sup>-1</sup> in spectrum B, and this is unequivocally demonstrated by their difference spectrum (trace C) in which the strong porphyrin band at 675 cm<sup>-1</sup> is completely canceled. Accordingly, the bands at 570 and 543 cm<sup>-1</sup> in spectra A and B are assigned to the <sup>16</sup>O<sub>2</sub>–Fe and <sup>18</sup>O<sub>2</sub>–Fe stretching modes, respectively. We note that these two frequencies are remarkably close to those of the wild-type oxyMb (571/544 cm<sup>-1</sup>).<sup>4d,h</sup>

Generally the  $\nu_{\text{Fe-CO}}$  and  $\nu_{\text{CO}}$  frequencies are very sensitive to amino acid replacements in the heme pocket.<sup>2c,e,g</sup> For example,  $\nu_{\text{Fe-CO}}$  of H64L Mb (490 cm<sup>-1</sup>) is significantly lower than that of the wild-type Mb (509 cm<sup>-1</sup>).<sup>2g</sup> In contrast, the  $\nu_{\text{Fe-O}_2}$  frequency of H64L oxyMb (570 cm<sup>-1</sup>) is insignificantly different from that of the wild-type oxyMb and native oxyHb (571 cm<sup>-1</sup>),<sup>4a–d</sup> while the Fe–His stretching frequencies of H64L (221 cm<sup>-1</sup>) and native (220 cm<sup>-1</sup>) deoxyMbs are practically the same.<sup>2g</sup> The same  $\nu_{\text{Fe-O}_2}$  frequency (571 cm<sup>-1</sup>)<sup>4g,h</sup> is seen for cytochrome *c* oxidase (CcO) in which a

(5) (a) Quillin, M. L.; Arduin, R. M.; Olson, J. S.; *J. Mol. Biol.* **1993**, 234, 140–155. (b) Springer, B. A.; Sliger, S. G.; Olson, J. S.; Phillips, G. N., Jr. *Chem. Rev.* **1994**, 94, 699–714. (c) Carver, T. E.; Brantley, R. E.; Singleton, E. W.; Arduini, R. M.; Quillin, M. L.; Phillips, G. N., Jr.; Olson, J. S. *J. Biol. Chem.* **1992**, 267, 14443–14450. (d) Quillin, M. L. Ph. D. Dissertation William Marsh Rice University, 1995.

(6) (a) Ogura, T.; Yoshikawa, S.; Kitagawa, T. *Biochemistry* **1989**, 28, 8022–8027. (b) Ogura, T.; Takahashi, S.; Hirota, S.; Shinzawa-Itoh, K.; Yoshikawa, S.; Appelman, E. H.; Kitagawa, T. *J. Am. Chem. Soc.* **1993**, 115, 8527–856.



**Figure 1.** (a) RR spectra in the 950–350  $\text{cm}^{-1}$  region for the  $^{16}\text{O}_2$  (A) and  $^{18}\text{O}_2$  (B) adducts of Leu-64 mutant Mb and their difference spectrum (C). (b) RR spectra in the 700–400  $\text{cm}^{-1}$  region for the  $^{16}\text{O}_2$  (A, C, and E) and  $^{18}\text{O}_2$  (B, D, and F) adducts of wild-type (A and B), Leu-29  $\rightarrow$  Phe (C and D) and Leu-29  $\rightarrow$  Trp (E and F) mutant Mbs, and their difference spectra [ $^{16}\text{O}_2$  minus  $^{18}\text{O}_2$ ; wild-type (G), L29F (H), and L29W (I)]. The ordinate scales in all the raw spectra are normalized with the intensity of porphyrin bands. Experimental conditions; (a) probe beam: 413.1 nm, 2 mW; pump beam: 406.7 nm, 20 mW at the sample; (b) excitation: 406.7 nm, 5 mW at the sample; accumulation time: 960 s (a) and 640 s (b) for each spectrum; sample: 10  $\mu\text{M}$  Mb (a) and 40  $\mu\text{M}$  (b) in 50 mM Na-phosphate buffer, pH 7.4.

Cu ion ( $\text{Cu}_B$ ) exists at 4.5 Å from the heme iron,<sup>7</sup> whereas the  $\nu_{\text{Fe}-\text{CO}}$  frequency of CcO ( $516 \text{ cm}^{-1}$ )<sup>8</sup> is significantly higher than those of other heme proteins.<sup>2a,c,g</sup>

Figure 1(b) displays the RR spectra in the 700–400  $\text{cm}^{-1}$  region for the  $^{16}\text{O}_2$  and  $^{18}\text{O}_2$  adducts of wild-type, L29F, and L29W Mbs excited at 406.7 nm and their difference spectra. The band at 571  $\text{cm}^{-1}$  for the  $^{16}\text{O}_2$ -bound wild-type Mb is shifted to 544  $\text{cm}^{-1}$  for the  $^{18}\text{O}_2$  adduct, in agreement with previously reported results.<sup>4d</sup> The  $\nu_{\text{Fe}-\text{O}_2}$  band of horse oxyMb was also observed at 571  $\text{cm}^{-1}$  under these conditions (data not shown). The corresponding band is at 568  $\text{cm}^{-1}$  for L29F Mb and at 574  $\text{cm}^{-1}$  for L29W Mb, their  $^{18}\text{O}_2$ -isotopic frequency shifts being more clearly seen in the difference spectra. The frequency shift between L29F and L29W Mb  $\nu_{\text{Fe}-\text{O}_2}$  bands is small,  $\sim 6 \text{ cm}^{-1}$ . The intensity changes of the  $\nu_{\text{Fe}-\text{O}_2}$  band are caused by differences in their  $\text{O}_2$  affinities (Table 1).

Comparison of the Fe– $\text{O}_2$  stretching frequencies, Fe–O–O bond angles, and the rate and equilibrium constants for  $\text{O}_2$  binding to wild-type, H64L, L29F, and L29W Mb are shown in Table 1. There is no correlation between  $\text{O}_2$  affinity,  $k'_{\text{O}_2}$ ,  $k_{\text{O}_2}$ , and  $\nu_{\text{Fe}-\text{O}_2}$ . Electrostatic interactions with His64 and Phe29 have little effect on the stretching frequency but produce large, 15–50-fold increases in  $K_{\text{O}_2}$ . There is a correlation between  $\nu_{\text{Fe}-\text{O}_2}$  and the Fe–O–O angle observed in the crystal structures of wild-type, L29F, and L29W MbO<sub>2</sub>. The L29F mutant shows the expected 120° angle, whereas the angles in the wild-type (118°) and native (116°) proteins appear to be slightly smaller,

(7) (a) Tsukihara, T.; Aoyama, H.; Yamashita, E.; Tomizaki, T.; Yamaguchi, H.; Shinzawa-Itoh, K.; Hakashima, R.; Yaono, R.; Yoshikawa, S. *Science* **1995**, *269*, 1069–1074. (b) Iwata, S.; Ostermier, C.; Ludwig, B.; Mitchel, H. *Nature* **1995**, *376*, 660–669.

(8) Hirota, S.; Ogura, T.; Shinzawa-Itoh, K.; Yoshikawa, S.; Nagai, M.; Kitagawa, T. *J. Phys. Chem.* **1994**, *98*, 6652–6660.

**Table 1.** Comparison of  $\nu_{\text{Fe}-\text{O}_2}$  ( $^{16}\text{O}_2$ ) and  $\text{O}_2$  Binding Parameters for Position 29 Mutants of Recombinant Sperm Whale Myoglobin at 20 °C, pH 7<sup>a</sup>

myoglobin	$\nu_{\text{Fe}-\text{O}_2}$ ( $\text{cm}^{-1}$ )	Fe–O–O angle	$k'_{\text{O}_2}$ ( $\mu\text{M}^{-1} \text{ s}^{-1}$ )	$k_{\text{O}_2}$ ( $\text{s}^{-1}$ )	$K_{\text{O}_2}$ ( $\mu\text{M}^{-1}$ )
wild-type	571	118 $\pm$ 4	17	15	1.1
H64L	570		98	4100	0.023
L29F	568	120 <sup>b</sup>	21	1.4	15
L29W	574	111	0.25	8.5	0.029

<sup>a</sup> The rate and equilibrium constants were taken from ref 5b, and the Fe–O–O angles for wild-type and L29F Mb from ref 5c. <sup>b</sup> From refs 5a and 5d and the estimated errors are  $\pm 4^\circ$ .

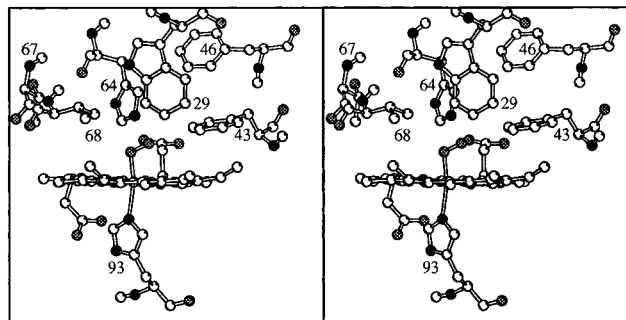


**Figure 2.** Stereoview of the distal pocket of sperm whale L29W MbO<sub>2</sub>.

although the observed differences are within the estimated error of  $\pm 4^\circ$ .<sup>5a,d</sup> The structure of L29W MbO<sub>2</sub> was determined for this work, and its active site is shown in Figure 2. The Fe– $\text{O}_2$  complex is clearly distorted by steric hindrance with the large indole side chain. The Fe–O–O angle is only 111°. The 9° difference between L29F and L29W MbO<sub>2</sub> corresponds with a 6  $\text{cm}^{-1}$  increase in  $\nu_{\text{Fe}-\text{O}_2}$ ; however, the changes in Fe–O–O angle are at the limits detectable by X-ray crystallography (Table 1). The weak inverse relationship between  $\nu_{\text{Fe}-\text{O}_2}$  and the Fe–O–O angle is probably due to kinematic effects on the molecular vibrations. In marked contrast to  $\nu_{\text{Fe}-\text{CO}}$ ,  $\nu_{\text{Fe}-\text{O}_2}$  shows no dependence on the electrostatic field adjacent to the bound ligand. The H64L mutation removes the positive field due to  $\text{N}_\epsilon\text{-H}$  of the distal imidazole, whereas the L29F mutation adds positive field due to the edge of the phenyl multipole. There is an  $\sim 40 \text{ cm}^{-1}$  difference between the  $\nu_{\text{Fe}-\text{CO}}$  values for these two mutants,<sup>2g</sup> whereas only a 2  $\text{cm}^{-1}$  difference is observed between the corresponding  $\nu_{\text{Fe}-\text{O}_2}$  values. The  $\text{Fe}^{\delta+}\text{-O-O}^{\delta-}$  system is highly polar, but the bond orders appear to be fixed with no alternative resonance structures. In contrast, the Fe–C–O system is apolar existing as an admixture of two alternative resonance structures involving net changes in bond order and alteration in the charge at the O atom:  $\text{Fe}^{\delta-}\text{-C}\equiv\text{O}^{\delta+}$  and  $\text{Fe}^{\delta+}=\text{C}=\text{O}^{\delta-}$ . Our results point out these important chemical differences between the Fe– $\text{O}_2$  and Fe–CO adducts and the differential effects of globin residues on the bond strengths and vibrational properties of these complexes.

**Acknowledgment.** This work was supported in part by U.S. Public Health Service Grants AR40252 (G.N.P.), GM35649 (J.S.O.), and HL47020 (J.S.O.), Grants C-1142 (G.N.P.) and C-612 (J.S.O.) from the Robert A. Welch Foundation, and the W. M. Keck Foundation, and Grant-in-Aid for Scientific Research on Priority Areas (Molecular Biometallics, 08249106) from the Ministry of Education, Science, Culture, and Sports Japan (T.K.). S.H. was supported by the fellowship of Japan Society for Promotion of Science for Junior Scientists.

JA9608297